桜島火山の噴煙柱の電気的・化学的性質

ブリストル大学地質学教室　ＳＪ，レイン
ランカスター大学環境科学・生物科学研究所
ＪＳ，ギルバート
ブリストル大学地質学教室　ＡＪ，ケンプ

本稿では 1990 年，1991 年および 1993～94 年の 3 回にわたり行った野外調査により得られた結果について述べる。噴煙柱から降下する，降雨または大気中の湿気による水滴は，多量の塩化物イオンおよび硫化物イオンを含み，低い pH 値を示した。これらのイオンの濃度は噴煙柱の拡散主軸から離れるにつれ減少する。ブルカノ式噴火の場合，噴煙柱から降下する火山灰粒子の表面は，大気中において獲得し得る最大値付近（$\pm 10^{-5}$ Cm^{-2}）まで帯電していることがわかった。また，大気中における電位勾配測定によって，火山灰粒子は負の電荷を，火山ガスからの水滴は正の電荷を運んでいることがわかった。爆発的噴火の際の電位勾配変動について簡単なモデル計算をした結果，火山ガスと火山灰は数十 m 離れ，それにより数クーロンの電荷が分離していることが示された。

Electrical and chemical properties of eruption plumes at Sakurajima volcano, Japan

SJ Lane[1], JS Gilbert[2] and AJ Kemp[1]
[1]Department of Geology, University of Bristol, Wills Memorial Building, Queens Road, Bristol BS8 1RJ, UK
[2]Institute of Environmental and Biological Sciences, Environmental Science Division, Lancaster University, Lancaster LA1 4YQ, UK

Abstract

We present data collected at Sakurajima volcano during three field seasons in 1990, 1991 and 1993/4. Liquid droplets falling from eruption plumes, either during periods of regional rainfall or high ambient humidity, were found to have a low pH and contain significant quantities of chlorine and sulphate ions. The concentration of these ions was found to decrease with increasing distance from the plume axis. The electrostatic charge on the surface of ash particles falling from plumes of Vulcanian style eruptions was shown to be close to the maximum sustainable ($\pm 10^{-5}$ C m^{-2}) in the atmosphere. Measurements of the atmospheric potential gradient showed that ash carries a net negative charge and liquid droplets, sourced from condensed volcanic and entrained gases, carries a net positive charge. A simple theoretical model of the evolving potential gradient during discrete explosive eruptions indicates separation of volcanic gases and ash by a few tens of meters and separation of a few Coulombs of charge.

1. Chemistry of liquid drops falling from eruption plumes

1. 1. Introduction

Observations of accretionary lapilli, spherical bodies of aggregated ash, falling from eruption plumes of Sakurajima volcano (Tomita 1985, Gilbert and Lane 1994) revealed the presence of both calcium sulphate and sodium chloride which had crystallised from solution onto the surfaces of ash particles. Accretionary lapilli formation is dependent upon the presence of hygroscopic phases (Gilbert and Lane 1994) to generate binding liquid layers. Samples of liquid fallout were collected and analysed in order to assess the chemical nature of liquids in the plume.

1. 2. Methods

Fallout collection bottles and lids were cleaned in nitric acid solution and rinsed in deionized water. In the field the bottles were placed on small raised platforms away from vegetation in order to reduce collection of splashed liquids. Liquid drops, containing small quantities of ash, were collected during a number of eruptions at Sakurajima over the course of several days in April 1991 and during periods of regional rainfall. Directly downwind of the vent the liquid drops falling from the plume were found, by using universal indicator paper, to have a pH of <1. Liquid drops, sometimes ash free, were also observed to fall in the absence of regional rainfall when the ambient humidity was high. The samples were sealed in the field prior to chemical analysis for chlorine and sulphate contents.

The liquid and ash were separated and sulphate and chlorine ion concentrations were determined using a Dionex model SP ion chromatograph. Separation was carried out on an anion column. The system was standardised using a three step calibration with 5, 10 and 20 mM solutions of both sulphate and chlorine ions. Standards and samples were diluted 100 fold with 18 MΩ water. 300 μL of samples and standards were injected via a sample port into a 100 μL loop and then transferred to the anion separation column. Separation took place and the unknown samples were plotted against the standard calibration graphs.

1. 3. Results and discussion

Figure 1 shows a plot of chlorine and sulphate ion contents of the liquid drops as a function of angle off the plume dispersal axis. The high chlorine and sulphate contents on the dispersal axis in comparison to those off the dispersal axis suggest that there was efficient scavenging of volcanic gases by the liquid drops. SEM observations of liquid drops on glass slides showed that calcium sulphate and sodium chloride crystals precipitated as the water evaporated. These crystals are likely to have formed due to reaction between the sulphate and chlorine ion rich liquids, originating from volcanic gases, and sodium and calcium within the volcanic ash.

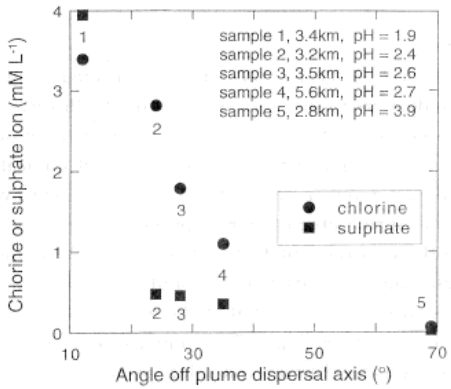

Figure 1. Chlorine and sulphate ion concentrations of liquids which fell through/from eruption plumes as a function of angle off the plume dispersal axis. Numbers next to data points are sample numbers. Sample collection distances from the vent and sample pH are indicated.

図 1. 噴煙柱からの水滴に含まれる塩化物および硫化物イオン濃度と噴煙の拡散方向からのずれの関係。プロットしたデータに添えた数字は試料番号を表わし，試料採取地点の火口からの距離と pH 値を併記した。

Rainfall through volcanic plumes will deposit highly acidic liquids on the underlying terrain. Precipitation of crystalline complexes from solution lead to enhanced concentrations of some minerals and this may have significant consequences for plant and animal life.

2. Measurement of electrostatic charge on falling volcanic ash

2. 1. Introduction

Evidence for electrical charging of volcanic ejecta is provided by the frequent observation of lightning (e.g. Mercalli 1907) during explosive volcanic eruptions. Laboratory experiments have shown that volcanic ash charges up during collision (Hatakeyama and Ucikawa 1952, Kikuchi and Endoh 1982). Aggregation plays a fundamental role in the fallout rates of fine volcanic ejecta (Carey and Sigurdsson 1982) and electrostatic charge may be important in particle aggregation processes in the absence of condensed liquids (Sorem 1982, Schumacher 1994, Gilbert and Lane 1994). Here we present measurements, previously reported in Gilbert et al. 1991, of

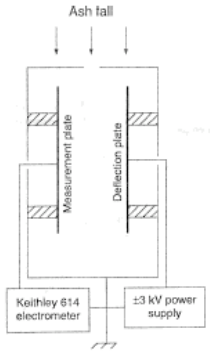

Figure 2. Schematic diagram of the apparatus used to measure the charge on ash falling from eruption plumes.
図 2. 降下火山灰の電荷量測定器の概念図。

electrostatic charge on ash particles falling from eruption plumes of Sakurajima volcano over a 16-day period in May 1990.

2. 2. Apparatus and methods

Figure 2 is a schematic representation of the apparatus used to collect and measure the bulk charge to mass ratio on ash falling from eruption plumes. Ash falling directly from the plume was allowed to enter a 5 mm wide slit and pass between two parallel copper plates mounted on PTFE insulators in an earthed case. The measurement plate was earthed *via* a Keithley 614 electrometer which monitored the charge flowing to or from the plate. The deflection plate was charged to ± 3 kV in order to generate an electric field of 1.2×10^5 V m^{-1} between the plates. Leakage currents across the insulators, or resulting from corona discharge within the apparatus, were only just detectable (<0.1 pA) under low humidity conditions, but increased noticeably (> 10 pA) as humidity increased. This is likely to have been due to formation of a thin layer of water on the insulators. The plates were lined with oil coated aluminium foil. Any ash with a small charge to mass ratio passed between the plates and fell to the base of the apparatus to be collected on oil coated aluminium foil. Ash with a significant charge to mass ratio was deflected by the electric field and collected on the oil film. The charge on ash adhering to the measurement plate was monitored by the electrometer and

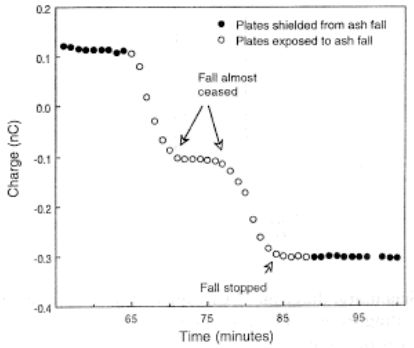

Figure 3. Data collected using the apparatus in Figure 2 showing the build-up of negative charge as volcanic ash collects on the measurement plate of the apparatus. Ambient humidity was 44%.
図 3. 図 2 の装置による測定結果。測定板に火山灰が集まるにつれて，負の電荷が集積していくことを示す。測定時の湿度は 44%であった。

was of the same sign as the potential applied to the deflection plate. After ash was allowed to fall between the plates the ash was removed from the oil film, degreased in a reflux still and weighed. The overall charge to mass ratio of the sample was then calculated. The size distribution of the samples was determined from silicon X-ray images using the Link Analytical Featurescan package.

2. 3. Results and discussion

Figures 3 and 4 are plots of charge against time for runs from two different explosive eruptions. Figure 3 shows data for a 100 minute run using a negatively charged deflection plate. In this experiment negatively charged ash was attracted to the measurement plate. The apparatus entrance slit was covered for 64 minutes so that the apparatus could stabilise. A light ash fall was then allowed to pass into the apparatus. This generated a negative gradient on the plot indicating the build-up of negatively charged ash on the measurement plate. The ash fall-rate was noticed to decrease almost to zero between 70-76 minutes into the run and the plot gradient is

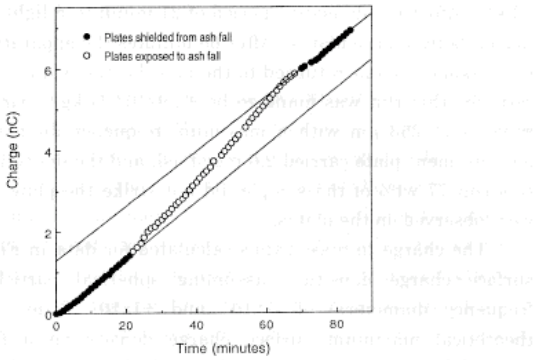

Figure 4. Data collected using the apparatus in Figure 2 showing the build-up of positive charge as volcanic ash collected on the measurement plate. Ambient humidity was 74% which explains the high background build-up of charge. The lines are linear best fits to the data collected when the apparatus was closed to ashfall.

図 4. 図 2 の装置による測定結果。測定板に火山灰が集まるにつれ、正の電荷が集積していくことを示す．測定時の湿度は 74%であったが，このような条件下では，火山灰の降下がなくても電荷量が増加するようである．実線は測定器を降下火山灰から遮蔽したときのデータの近似直線を示す。

almost zero during this time. This provides evidence that the measured charge had originated from the ash falling through the apparatus rather than from a leakage current. Between 76 and 84 minutes light ash fall resumed and the plot gradient became negative. After 84 minutes the ash fall ceased and the apparatus was covered. The plot gradient then returned to background levels. The charge to mass ratio for this run was calculated to be -2.7×10^{-4} Ckg^{-1}. Grain size ranged from 0.9 to 152 μm with a maximum frequency diameter of 55 μm. The measurement plate carried 1.5 mg of ash and the deflection plate 0.5 mg. In this run 93 wt% of the ash entering the apparatus did not strike the plates and therefore had insufficient charge to mass ratio to contact the plates. No aggregates were observed adhering to the plates indicating that aggregates had insufficient charge to mass ratio to be deflected. This provides evidence that a large proportion (up to 93 wt% ?) of the ash falling into the apparatus did so in aggregated form.

Figure 4 shows data for a run in which the deflection plate was held at +3 kV. After a stabilisation period of 21 minutes, a light ashfall was allowed to pass between the plates. After 68 minutes the apparatus was shielded and the leakage current returned to the precollection value. The charge to mass ratio for this run was found to be $+4.9 \times 10^{-4}$ C kg^{-1}. Grain size was in the range 1 to 253 μm with a maximum frequency diameter of 49 μm. The measurement plate carried 2.6 mg of ash and the deflection plate 3.7 mg. In this run 77 wt% of the sample did not strike the plates and no aggregates were observed on the plates.

The charge to mass ratios calculated for data in Figures 3 and 4 yield surface charge densities (assuming spherical particles and maximum frequency diameters) of -7×10^{-6} and $+1 \times 10^{-5}$ C m^{-2} respectively. The theoretical maximum surface charge density on a flat surface in the atmosphere is $\pm 2.6 \times 10^{-5}$ C m^{-2}, above which air breakdown occurs. For all practical purposes the maximum charge per unit area that can be carried by a stream of insulating particles is $\pm 1 \times 10^{-5}$ C m^{-2} (Blythe and Reddish 1979). The ash particles generated during explosive volcanic activity at Sakurajima thus appear to be charged almost to the air ionisation limit, that is they are nearly saturated with charge.

There are a number of possible mechanisms for the origin of charged particles in the Sakurajima eruption plumes. Charge transfer occurs when two materials of different surface work function are separated. This is known as the triboelectric effect. Such a mechanism may occur during the separation of glass and crystals during magma fragmentation and from collisions within the plume. It is well known that charge transfer and the generation of ions takes place during the deformation (Enomoto and Hashimoto 1990) and fracture (Donaldson et al. 1988) of materials. It is proposed that this phenomenon (fractoemission or fractocharging) plays a significant role in charge generation during the fragmentation of magma into volcanic ejecta. The interaction of water (Walker 1973, Walker and Croasdale 1972) may enhance the generation of charge indirectly by substantially increasing the degree of fragmentation of the magma.

3. Atmospheric electric potential gradient changes measured during explosive eruptions

3.1. Introduction

All atmospheric clouds produce electrical perturbations because their electrical properties are different to those of clear air. In general these perturbations are so small that it is impossible to recognise the external electric fields of clouds against the normal variations of the electric field of the surrounding cloudless atmosphere. The exception to this is the thunder cloud which is capable of producing electric fields sufficiently large to result in electric sparks many kilometres in length. Electric potential gradient measurements made during fair weather, beneath clouds, during rain and snowfall and at the coast are available (Chalmers 1967). Charge distributions have also been described in non-raining clouds (Whitlock and Chalmers 1956) and in dust devils (Freier 1960, Crozier 1964). Positively and negatively charged particles in a volcanic plume can carry sufficient charge to cause attraction between particles and form ash clusters (Sorem 1982, Gilbert et al. 1991, Schumacher 1994). However, the distribution of charge within volcanic plumes is not well understood and electric potential gradient data from explosive eruptions are scarce. Hatakeyama and Uchikawa (1952) interpreted the plume from Aso volcano, Japan to be dominated by positive charge in its lower and negative charge in its upper regions. Kikuchi and Endoh (1982) measured atmospheric electric potential gradient changes from wind blown volcanic ash and ash plumes at Usu volcano, Japan. Anderson et al. (1964) found the plume from Surtsey volcano, Iceland to be dominated by positive charge in its upper and negative charge in its lower region, the inverse of that found at Aso. This perhaps being due to different mechanisms of ash plume generation between these two volcanoes. We present field measurements of the effects of explosive eruptions at Sakurajima volcano on the local atmospheric electric potential gradient (Lane and Gilbert 1992, Lane 1994).

3. 2. Apparatus and methods

Vertical electric potential gradients were measured using JCI rotating vane fieldmeters (Chubb 1990) mounted on short masts. This arrangement resulted in a noise free enhancement of the field by a factor of approximately 20. The fieldmeters were either oriented so that the aperture was facing upwards for attended fieldmeters or downwards for unattended

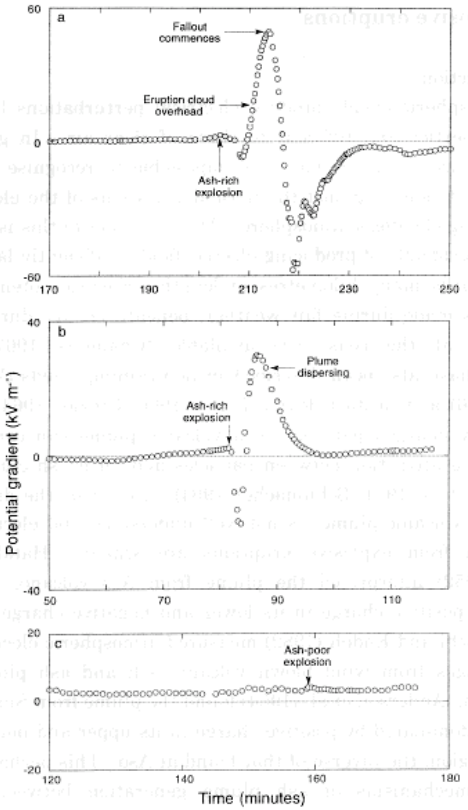

Figure 5. Potential gradient verses time for three explosive events. **a** Ash-rich explosion at 13:39 JST on 3 May 1991 with the fieldmeter located downwind of the vent. **b** Ash-rich explosion at 10:16 JST on 30 April 1991 with the fieldmeter approximately 70° off the plume axis. **c** Ash-free explosion at 15:44 JST on 30 April 1991 with fieldmeter on the plume dispersal axis.

図 5. 爆発に伴う電位勾配の時間変化。 **a** 1991 年 5 月 3 日 13 時 39 分の火山灰の多い爆発。測定器を火口の風下側に設置した。 **b** 1991 年 4 月 30 日 10 時 16 分の火山灰の多い爆発。測定器を噴煙の拡散主軸と 70°の角度をなす方向に設置した。 **c** 1991 年 4 月 30 日 15 時 44 分の火山灰の少ない爆発。測定器を噴煙の拡散していく方向に設置した。

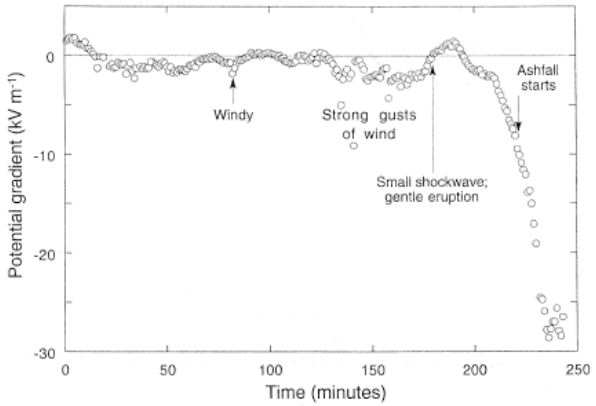

Figure 6. Potential gradient verses time during ashfall on 25 March 1991
図 6. 1991 年 3 月 25 日の降灰に伴う電位勾配の時間変化

fieldmeters. Data plotted in Figures 5, 6, 7 and 8 are the measured values i.e. 20x ground level values. In the field data were either logged manually when only one fieldmeter was in use (Lane and Gilbert 1992) or automatically by means of dataloggers when an array of fieldmeters was used (Lane 1994).

3. 3. Results

Figure 5 shows electric potential gradient data collected by single fieldmeters for three separate eruptions. Figure 5a shows data collected near the Arimura lava observatory, 2.75 km SSE and downwind of the vent, i.e. on the plume axis. 206 minutes into the run a loud detonation was heard (followed by metre sized bombs being ejected from the crater) after which a dark ash laden cloud ascended to a height of approximately 2.5 km above the crater rim. Six minutes after the explosion fallout of <1 cm diameter particles commenced at the measurement site. Figure 5b shows data collected from a locality 2 km SW of the vent with a wind direction of NNW, i.e. off plume axis. After 82 minutes a loud detonation was heard, at which

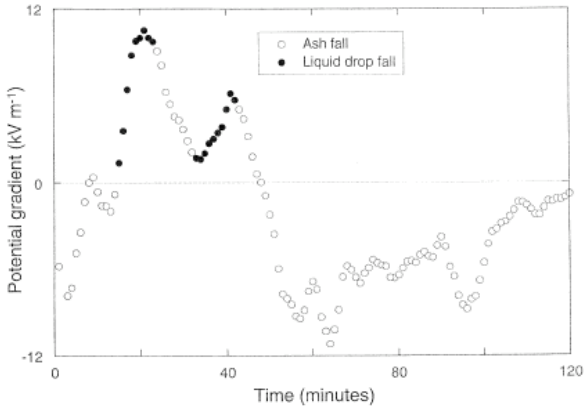

Figure 7. Potential gradient verses time during ash and acid liquid fall on 27 April 1991
図 7. 1991 年 4 月 27 日の火山灰および酸性の水滴の降下に伴う電位勾配の時間変化

time a dark ash laden plume ascended approximately 1.5 km above the crater rim. No ash fall occurred at the measurement locality. Figure 5c shows data collected at the same locality as that of Figure 5a and downwind of the vent. After 159 minutes a loud detonation was heard after which a white plume rose approximately 1.5 km above the crater rim. No ash was observed to fall from this plume.

Figure 6 shows the effect of ashfall on the potential gradient. These data were collected at a locality 3.5 km E and downwind of the vent. During the early stages of monitoring the volcano was emitting white plumes up to 300 m high. Fluctuations in the measured potential gradient were noted when strong winds blew dust clouds over the measurement site. After 180 minutes a weak detonation was heard and an ash laden plume ascended approximately 500 m above the vent. Light ashfall commenced 39 minutes later. Figure 7 shows the effect of both ashfall and plume-induced acid rainfall. The data were collected 2.25 km NW and downwind of the vent, on an overcast day on which there was no regional rainfall. Sakurajima was

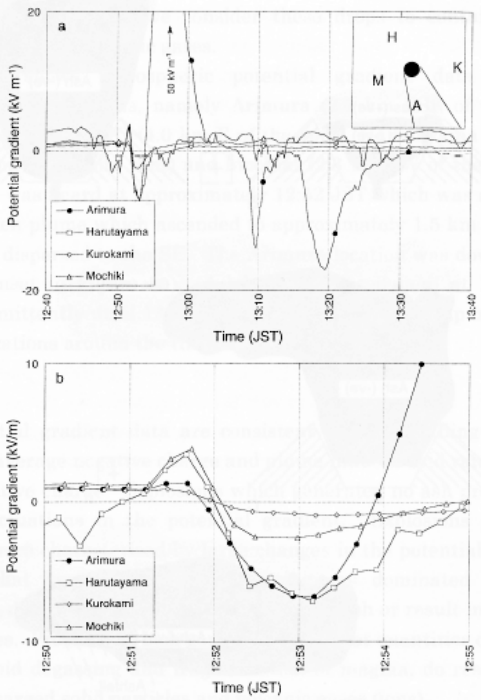

Figure 8. Potential gradient verses time for an explosive ash-rich eruption at 12:52 JST on 27 December 1993. **a** Data collected simultaneously by four fieldmeters. The inset indicates the relative locations of fieldmeters, vent and plume. **b** Expanded version of Figure 8a showing the details of changes in potential gradient at the onset of eruption measured at all four locations.

図 8. 1993 年 12 月 27 日 12 時 52 分の火山灰の多い爆発に伴う電位勾配の時間変化。**a** 4 地点における同時測定。枠内の図は測定点、火口および噴煙の拡散の相対位置関係を示す。 **b** 噴火の始まりの部分について図 8a を拡大したもの。

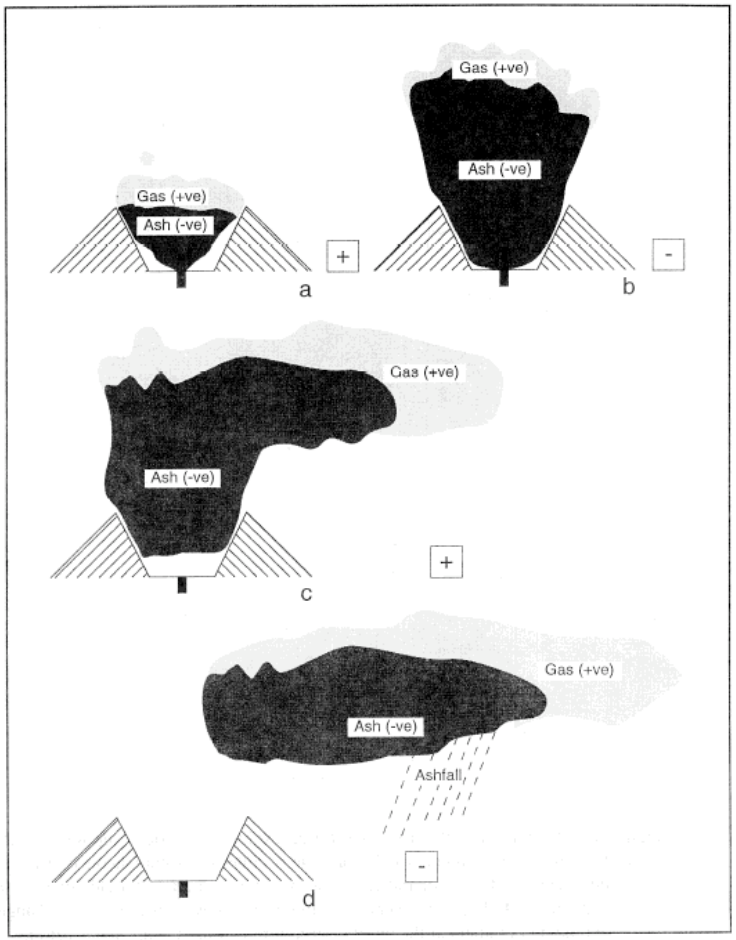

Figure 9. Schematic representation of growth and dissipation of an eruption plume consistent with the observed potential gradient data

図 9. 観測された電位勾配を説明するための噴煙柱の成長・散逸の概念的モデル

erupting a small plume (< 300 m high). A light fall of mainly ash clusters (<2 mm in diameter) occurred for the duration of measurement. Between the periods 15-22 and 32-41 minutes ash poor liquid drops also fell. These were found to have a pH < 1 when tested with universal indicator paper. On account of the very low pH we consider these drops to contain a high proportion of condensed volcanic gases.

Figure 8a shows atmospheric potential gradient data collected simultaneously at 4 locations, namely Arimura (2.7 km SSE of the vent), Kurokami branch of the SVO (4.0 km E of the vent), Harutayama branch of the SVO (2.7 km NW of the vent) and Mochiki (2.3 km SW of the vent). A loud detonation was heard at approximately 12:52 JST which was associated with an ash laden plume which ascended to approximately 1.5 km above the crater wall and dispersed to the SE. The Arimura location was downwind of the vent (see inset in Figure 8a). Ashfall commenced here at 12:56 and continued intermittently until 13:32. Figure 8b shows a close-up of the data from all four locations around the time of the eruption.

3. 4. Discussion

The potential gradient data are consistent with ash falling from the plume with an average negative charge and plume induced acid rain carrying an average positive charge. Explosions which generated no ash produced no measurable fluctuations in the potential gradient. Explosions producing abundant ash were characterised by large changes in the potential gradient. This implies that lava dome collapse during gas dominated eruptions (Ishihara 1985), does not generate large amounts of ash or result in potential gradient changes. Processes which generate significant quantities of fine ash, such as the rapid degassing and fragmentation of magma, do result in the generation of charged solid particles and volcanic gases (ions).

Explosive eruptions resulting in ash generation exhibit a sequence of potential gradient reversals. These reversals may be explained qualitatively by assigning an average negative charge to ash particles and an average positive charge to the erupted gases. Figure 9 shows one series of possible explanations for the potential gradient reversals. In the early stages of an eruption (Figure 9a) positively charged volcanic gases separate from the top of the buoyant plume, the separation being enhanced by particle aggregation increasing the fall velocities of small particles (Lane et al. 1993). At Sakurajima this charged gas cloud emerges first from the 300 m deep crater and becomes 'visible' to the fieldmeters prior to the ash plume. It is this gas

cloud which generates the small positive potential gradient shown by all fieldmeters regardless of position around the volcano (Figures 5a, b and 8b). As the column ascends (Figure 9b) the negatively charged ash-rich lower regions of the column dominate the measured potential gradient at which point all fieldmeters show a negative potential gradient (Figures 5a, b and 8a, b). The plume is then distorted by the prevailing wind (Figure 9c). The potential gradient measured during this period depends on the relative positions of the fieldmeter and the plume. In this way different potential gradients are measured by fieldmeters located around the volcano. For example higher wind speeds at greater altitudes carry the positively charged gases over any downwind fieldmeters and this produces a large positive potential gradient (Figures 5a and 8a, b). This may also be detected by fieldmeters at up to 70° to the plume axis (Figure 5b). However, fieldmeters upwind of the plume see a reducing negative potential gradient (Figure 8b) as the plume recedes from the fieldmeter in the prevailing wind. The plume continues to travel over the downwind fieldmeters and, with time, they detect the average negative charge on the ash laden part of the plume (Figure 9d), particularly when ash fallout occurs. As the eruption switches off and the plume recedes from the vent all fieldmeters return to measuring the pre-eruption ambient levels of atmospheric potential gradient (Figures 5 and 8).

The ability for a fixed array of fieldmeters around the volcano to yield data on the travel direction and areas of ash fallout is shown by Figure 8. The initial positive increase in potential gradient shown simultaneously by all fieldmeters in the array may be correlated with the emergence of the first volcanic ejecta (gases) of an ash bearing eruption to appear above the crater rim. The characteristic large positive potential gradient subsequently exhibited by fieldmeters in the plume propagation direction allows rapid detection of plume orientation in the absence of both wind direction data at the relevant altitude and direct visual data. The subsequent large negative potential gradients in the downwind direction indicate that ash is falling in these regions. Electric potential gradient monitoring may therefore be used as a remote sensor of volcanic eruptions.

3. 5. Theory

Using simple theoretical descriptions of the potential gradient of a charge dipole it is possible to qualitatively reproduce some of the features of the measured potential gradient data. The potential, V, of a point distance r from a charge Q is,

$$V = \frac{Q}{4\pi\varepsilon r} \tag{1}$$

where ε is the permittivity of free space. In Cartesian co-ordinates $r = \sqrt{\Delta x^2 + \Delta y^2 + \Delta z^2}$, where Δx, Δy and Δz are the x, y, and z co-ordinate differences between the charge position and the point of potential measurement. Let (x, y, z) be the measurement position and points $(x_1, y_1, z_1), (x_2, y_2, z_2)$ etc. be positions of charges. The potential gradient is given by,

$$\nabla V = \frac{dV}{dr}\mathbf{r} \tag{2}$$

or, in Cartesian co-ordinates,

$$\nabla V = \frac{dV}{dx}\mathbf{x} + \frac{dV}{dy}\mathbf{y} + \frac{dV}{dz}\mathbf{z} = \mathbf{V}_x + \mathbf{V}_y + \mathbf{V}_z \tag{3}$$

The co-ordinate system is defined as z being vertical with +ve upwards and the ground in the xy plane. Substituting for r in (1) and differentiating with respect to x gives,

$$\frac{dV}{dx} = \frac{Q}{4\pi\varepsilon\left(D_x^2 + D_y^2 + D_z^2\right)^{1/2}} \frac{d}{dx} \tag{4}$$

and likewise for dV/dy and dV/dz. Differentiating yields the potential gradients along the x, y, and z directions,

$$\mathbf{V}_x = \frac{Q}{4\pi\varepsilon} \frac{-D_x\mathbf{x}}{\left(D_x^2 + D_y^2 + D_z^2\right)^{3/2}}$$
$$\mathbf{V}_y = \frac{Q}{4\pi\varepsilon} \frac{-D_y\mathbf{y}}{\left(D_x^2 + D_y^2 + D_z^2\right)^{3/2}} \tag{5}$$

$$\mathbf{V}_z = \frac{Q}{4\pi\varepsilon} \frac{-D_z\mathbf{z}}{\left(D_x^2 + D_y^2 + D_z^2\right)^{3/2}}$$

Let measurements take place on the ground i.e. where $z = 0$. Co-ordinates of the measurement point are therefore $(x, y, 0)$. With one charge at (x_1, y_1, z_1) in the atmosphere there is an image charge at $(x_1, y_1, -z_1)$. Using the principle of superposition and equation (3) for both charges the potential gradient for one atmospheric charge measured from a flat conducting earth is given by

$$\nabla V_1 = \frac{Q}{2\pi\varepsilon} \frac{z_1\mathbf{z}}{\left((x-x_1)^2 + (y-y_1)^2 + z_1^2\right)^{3/2}} \tag{6}$$

For dipole charges the total ground level potential gradient is given by the vector addition of the potential gradient generated by each point charge or charge centre thus

$$\nabla V = \nabla V_1 + \nabla V_2$$
$$= \frac{Q}{2\pi\varepsilon}\left(\frac{z_1\mathbf{z}}{\left((x-x_1)^2 + (y-y_1)^2 + z_1^2\right)^{3/2}} + \frac{z_2\mathbf{z}}{\left((x-x_2)^2 + (y-y_2)^2 + z_2^2\right)^{3/2}}\right) \tag{7}$$

Using an equation relating charge centre position to time, calculations can be made of simple potential gradient changes as a function of time. The evolution of potential gradient during short-lived explosive eruptions has been postulated in Figure 9. In the first instance positive and negative charges emerge from the vent unseparated. The charges then separate vertically as the thermally buoyant plume develops within the crater. The plume is then angled over in the prevailing wind becoming horizontal as it approaches neutral buoyancy in the atmosphere. The evolution of the potential gradient may be considered in terms of two models for the undeformed initial plume and the wind deformed plume. We consider these below.

3.5.1. Evolving vertical dipole (undeformed plume)

The atmospheric potential gradient data for ash-rich explosive eruptions all show a small positive peak followed by a small negative peak regardless of the position of the measurement locality and the direction of the prevailing wind (Figure 5a, b and 8b). These peaks may, therefore, be due to charge separation before the wind has had a significant distorting

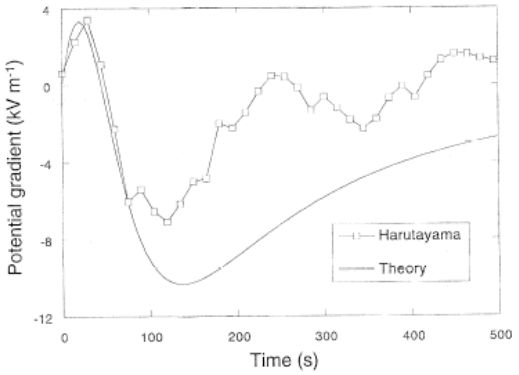

Figure 10. Potential gradient verses time for a simple theoretical evolving vertical dipole compared with measured data from Harutayama of Figure 8b
図 10. 鉛直方向のダイポールモデルに基づく電位勾配の時間変化の理論値とハルタ山における観測データ（図 8b）の比較

effect on the plume. A simple theoretical model assumes that the plume charge centres (gas and ash) are coincident at time zero and 2000 m horizontal and 500 m vertical distance from the fieldmeter. The gas, which carries an average positive charge, is assigned a vertical velocity of 20.5 m s^{-1} and the ash, which carries an average negative charge, 20 m s^{-1}. We consider the separation velocity of gas and ash (0.5 m s^{-1}) to be reasonable because most sub-100μm ash particles are efficiently scavenged into aggregates which have fall velocities considerably higher that the single particles (Lane et al. 1993). Figure 10 shows a plot of the theoretical potential gradient with time compared to the measured up-wind data for Harutayama from Figure 8b. The theoretical data have been multiplied by 20 to scale for the mast mounting of the fieldmeter. A net charge of 10 C for both gas and ash was found to produce reasonable agreement between theory and measured data for the first 100 s. During this period the plume will have ascended in excess of 1 km. At 1 km altitude it is likely that the plume will be significantly distorted by the prevailing wind resulting in a reduction of the measured potential gradient as the plume recedes from the fieldmeter (Figure 10).

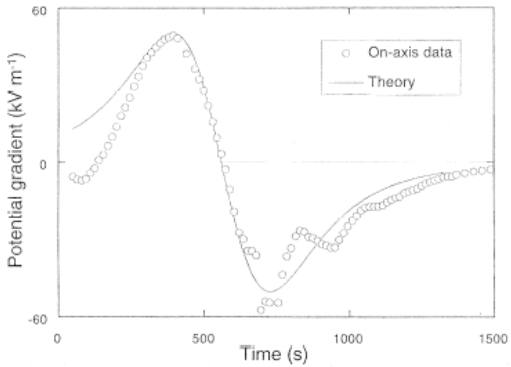

Figure 11. Potential gradient verses time for a simple horizontal dipole theoretical model compared with the field data of Figure 5a
図 11. 水平方向のダイポールモデルに基づく理論値と電位勾配の時間変化の測定値（図 5a）の比較

3. 5. 2. Horizontal dipole (wind deformed plume)

The qualitative model for potential gradient changes detected by on-axis fieldmeters is shown in Figure 9c, d and can crudely be represented as a horizontal dipole in the atmosphere. Figure 11 shows a plot derived from equation (7) with the measured on-axis data from Figure 5a plotted for comparison. A wind speed of 6 m s^{-1} was required to match the wavelengths of the theoretical and measured data. The approximate horizontal velocity of this plume may be estimated from the vent to measurement locality distance of 2.75 km and the time between eruption and first fallout of six minutes to be 7.6 m s^{-1}. Using a charge of 10 C, as above, and a fieldmeter to plume height of 2000 m a horizontal gas and ash plume separation of 130 m provided a reasonable fit between measured data and theory. The theoretical data are multiplied by 20 to account for the amplification of the measured signal due to mast mounting. The on-axis data (Arimura) from Figure 8a do not fit the horizontal model as well on account of the large height differences between positive and negative potential gradient peaks. This illustrates the complicated effects of plume dynamics and prevailing weather conditions on the generated potential gradient.

Combination of the evolving vertical dipole (Figure 10) and the horizontal dipole (Figure 11) models provides, to a first approximation, a reasonable description of the measured atmospheric electric potential gradients during explosive ash-rich eruptions at Sakurajima. The quantity of charge required by the theory to be separated is between a few to a few tens of Coulombs. This is similar to typical charge values discharged by lightning in thunder clouds (Vonnegut 1973). The input of realistic horizontal and vertical velocity values and charge levels, together with acceptable separation distances for the ash and gas plume charge centres at Sakurajima, provides confidence in this simple model.

4. Conclusions

Explosive eruptions at Sakurajima volcano generate large perturbations in the atmospheric electric potential gradient. These are potentially useful for monitoring purposes. The potential gradient changes are caused by the generation followed by the separation of volcanic ash and gases. At Sakurajima ash takes on average negative and gases average positive charge. The volcanic gases condense, and together with condensed entrained water, deposit highly acidic liquids on the surrounding countryside. The liquids with the lowest pH fall directly downwind of the vent.

Acknowledgements

We gratefully acknowledge the support of Professor K Kamo, Dr K Ishihara, Dr M Iguchi, Mr T Eto and the staff of the Sakurajima Volcanological Observatory. We thank Dr JN Chubb for advice on potential gradient measurement methods. SJL thanks the Royal Society for two Japanese study visit grants and a small equipment grant. JSG thanks the NERC for a research fellowship.

References

Anderson R, Bjornsson S, Blanchard DC, Gathman S, Hughes J, Jonasson S, Moore CB, Survilas HJ, Vonnegut B (1964) Electricity in volcanic clouds. Science 148:1179-1189

Blythe AR, Reddish W (1979) Charges on powders and bulking effects. Inst Phys. Conf Ser 48: 107-124

Carey SN, Sigurdsson H (1982) Influence of particle aggregation on deposition of distal tephra from the May 18, 1980 eruption of Mount St. Helens' volcano. J Geophys Res 87(B8): 7061-7072

Chalmers JA (1967) *Atmospheric electricity*. Pergamon Press, London

Chubb JN (1990) Two new designs of 'field mill' type fieldmeters not, requiring earthing of rotating chopper. IEEE Trans Ind Applic 26:1178-1181

Crozier WD (1964) The electric field of a New Mexico dust devil. J Geophys Res 69:5427-5429

Donaldson EE, Dickinson JT, Bhattacharya SK (1988) Production and, properties of ejecta released by fracture of materials. J Adhesion 25: 281-302

Enomoto Y, Hashimoto H (1990) Emission of charged particles from indentation fracture of rocks. Nature 346: 641 643

Freier GD (1960) The electric field of a large dust devil. J Geophys Res 65:3504

Gilbert JS, Lane SJ, Sparks RSJ, Koyaguchi T (1991) Charge measurements, on particle fallout from a volcanic plume. Nature 349: 598-600

Gilbert JS, Lane SJ (1994) The origin of accretionary lapilli. Bull Volcanol 56: 398-411

Hatakeyama H, Uchikawa K (1952) On the disturbance of the atmospheric, potential gradient caused by the eruption-smoke of the volcano, Aso. Pap Met Geophys Tokyo 2: 85-89

Ishihara KJ (1985) Dynamical analysis of volcanic explosion. J Geodynamics 3:327-349

Kikuchi K, Endoh T (1982) Atmospheric electrical properties of volcanic ash, particles in the eruption of Mt. Usu volcano, 1977. J Met Soc Japan 60: 548-561

Lane SJ (1994) Logit: User-friendly data logging. Terra Nova 6(2):202

Lane SJ, Gilbert JS (1992) Electric potential gradient changes during, explosive activity at Sakurajima volcano, Japan. Bull Volcanol 54: 590-594

Lane SJ, Gilbert JS, Hilton M (1993) The aerodynamic behaviour of volcanic, aggregates. Bull Volcanol 55: 481-488

Mercalli G (1907) *I Vulcani Attivi della Terra*, 421 (Ulrico Hoepli, Milan)

Schumacher R (1994) A reappraisal of Mount St Helens' ash clusters - depositional model from experimental observation. J Volcanol Geotherm Res 59: 253-260

Sorem RK (1982) Volcanic ash clusters: tephra rafts and scavengers. J Volcanol Geotherm Res 13: 63-71

Tomita K, Kanai T, Kobayashi T, Oba N (1985) Accretionary lapilli formed by the eruption of Sakurajima volcano. J Japan Assoc Min Petr Econ Geol 80: 49-54

Vonnegut B (1973) Atmospheric electrostatics. Ch 17 in *Electrostatics and its applications* Moore AD (ed) Wiley Interscience

Walker GPL (1973) Explosive volcanic eruptions - a new classification scheme. Geol Rundsch 62: 431

Walker GPL, Croasdale R (1972) Characteristics of some basaltic pyroclastics. Bull Volcanol 35: 303-317

Whitlock WS, Chalmers JA (1956) Short period variations in the atmospheric electric potential gradient. Quart J R Met Soc 82: 325-326

(Received on March 10, 1995)